Crystallization of running filament in melt spinning of polypropylene

O. Ishizuka and K. Koyama
Faculty of Engineering, Yamagata University, 4-3-16 Jyonan, Yonezawa, 992, Japan
(Received 5 October 1976; revised 15 March 1977)

The crystallization kinetics of the running filament in melt spinning have been studied for three cases: isothermal crystallization of an isotropic melt, non-isothermal crystallization of an isotropic melt, and non-isothermal crystallization of a non-isotropic melt. Both the temperature and the orientation dependences of nucleation rate and growth rate are estimated for polypropylene. Calculated curves for non-isothermal crystallization of a non-isotropic melt with partial high orientation closely approximate the experimental data. In particular, the experimental data are best explained by crystallization with two-dimensional growth. The crystallization processes in melt spinning may be governed by localized molecular orientation of the supercooled melt in the initial stage.

INTRODUCTION

Generally, solidification during the melt spinning of crystallizable polymer is non-isothermal crystallization of a non-isotropic melt. Little work has been reported on the kinetics of crystallization of the running filament in melt spinning because here crystallization is very much faster than isothermal crystallization of the isotropic state. However, many papers have reported on the isothermal crystallization of isotropic melts. Non-isothermal crystallization of an isotropic melt has been studied by several investigators. Comparison of theory and experiment has been reported on the variation of crystallinity of as-spun filaments[1,2], on the crystallization of poly(ethylene terephthalate) using differential thermal analysis[3], and on the crystallization of polyethylene using X-ray diffraction[4–6]. On the other hand, in isothermal crystallization of a non-isotropic melt, the molecular orientational effect on rate of crystallization is significant. The increase in crystallization rate can be divided into two parts, nucleation rate and growth rate; it has been theoretically estimated for molten polyethylene subjected to a constant shear stress[7].

In this work, the changes of crystallinity and of non-crystalline orientation along the spinning direction were measured. The results relate to three cases: isothermal crystallization of an isotropic melt, non-isothermal crystallization of an isotropic melt, and non-isothermal crystallization of a non-isotropic melt. Data on nucleation rate and growth rate are required for the study of the kinetics as functions of crystallization temperature and non-crystalline orientation. The temperature dependence of nucleation rate and growth rate for polypropylene (PP) was derived from many data on isothermal crystallization[22–27]. The orientation dependence of these was also calculated.

THEORY

We start from the theory of phase transformations proposed by Avrami[8,9] and Mandelkern *et al.*[10]. According to this theory the degree of transformation at time t amounts to:

$$-\ln\left(1-\frac{X}{X_\infty}\right)=\frac{1}{X_\infty}\frac{\rho_c}{\rho_l}\int_0^t \nu(t,\tau)\dot{N}(\tau)\mathrm{d}\tau \tag{1}$$

$$\nu(t,\tau)=k_f\left[\int_\tau^t G(u)\mathrm{d}u\right]^n$$

Here X_∞ is crystallinity at the termination of the crystallization process, ρ_c and ρ_l are the density of the crystalline and liquid phase, respectively, $G(u)$ is the rate of linear growth at time u, $\dot{N}(\tau)$ is the rate of nucleus formation at time τ, k_f is the shape factor and n is a constant.

Usually, in isothermal crystallization from an isotropic melt, one assumes that G and $\dot{N}$ are constants. This assumption reduces equation (1) to:

$$-\ln\left(1-\frac{X}{X_\infty}\right)=\frac{1}{X_\infty}\frac{\rho_c}{\rho_i}Kt^n \tag{2}$$

In this case, the crystallization kinetics can be analysed by Avrami plotting ($\ln[-\ln(1-X/X_\infty)]$ against $\ln t$).

In non-isothermal crystallization from a non-isotropic melt, G and $\dot{N}$ are dependent on the crystallization temperature (T) and the molecular orientation of non-crystalline liquid (Δn_a), which are functions of time in the melt-spinning process. That is to say, the rate of nucleus formation at time τ from the spinneret is $\dot{N}[T(\tau), \Delta n_a(\tau)]$, and the rate of linear growth at time u from the spinneret is $G[T(u), \Delta n_a(u)]$. Then we may consider that the nucleus which was originated at time τ is growing up to observed time t ($= p\Delta t$) with the various linear growth rate of $G_j[T(u), \Delta n_a(u)]$. Here p is the number of time intervals Δt. In this case the degree of crystallinity X at time t along the spinning path can be obtained as the following expressions by analogy with equation (1). For a homogeneously nucleated system:

$$-\ln\left(1-\frac{X}{X_\infty}\right)=\frac{1}{X_\infty}\frac{\rho_c}{\rho_l}k_f\sum_{i=0}^{p}\times$$

$$\left\{\sum_{j=i}^{p}G_j[T(u),\Delta n_a(u)]\,\Delta t\right\}^n \dot{N}_i[T(\tau),\Delta n_a(\tau)]\,\Delta t \qquad (3)$$

For a heterogeneously nucleated system:

$$-\ln\left(1-\frac{X}{X_\infty}\right)=\frac{1}{X_\infty}\frac{\rho_c}{\rho_l}k_f\sum_{i=0}^{p}\times$$

$$\left\{\sum_{j=i}^{p}G_j[T(u),\Delta n_a(u)]\,\Delta t\right\}^n \bar{N}_i[T(\tau),\Delta n_a(\tau)] \qquad (4)$$

Additionally, in non-isothermal crystallization from an isotropic melt, G and $\dot{N}$ are dependent on crystallization temperature and independent of orientation. Therefore, $X(t)$ is calculated assuming that $\Delta n_a(t)$ at time t may be zero in equation (3) or (4).

EXPERIMENTAL

The sample used in this study was commercial polypropylene of intrinsic viscosity $[\eta]$ = 2.2 dl/g determined in decalin at 135°C. The polymer melt was extruded at 250°C by a regulated constant nitrogen pressure through a die fitted with a single orifice. The die diameter was 2 mm, extrusion rate 0.4 g/sec and stretch ratio 59 or 240. The extruded fibre was passed through a diffractometer with a rotating-anode X-ray generator and was wound onto a take-up device with speed of 10 m/min or 40 m/min. Wide-angle X-ray diffraction patterns were obtained along the spinning path to a distance of 100 cm from the spinneret. In this measurement, the X-ray was conducted on the moving filament during processing. CuKα radiation through a Ni filter was used. The working conditions were 40 kV, 100 mA. The separation of amorphous scattering from the crystalline peaks was made by the method suggested by Natta *et al.*[11]. Data on the crystal orientation and the degree of crystallinity were obtained from (110), (040) and (111) reflections. The X-ray diffraction curve at a distance of 100 cm from the spinneret was almost the same as that of the take-up filament. The degree of crystallinity of the take-up filament, derived from density measurement, was 60%. The running filament was photographed through the microscope at magnifications of 100x and the diameter d determined.

The temperature distribution was evaluated using Ziabicki's procedure[12]. The time from the spinneret was calculated from the diameter profile

$$t=\int_0^x 1/V\mathrm{d}x=\pi/4Q\int_0^x d^2\mathrm{d}x$$

The birefringence of the running filament was measured as a function of position along the spinning path. The birefringence was determined by measurement in a polarization microscope using a Bereck compensator. Both the crystalline and non-crystalline components of a polymer contributed to the measured birefringence. The molecular orientation of the non-crystalline component (Δn_a) was estimated from a combination of the X-ray diffraction measurement with the birefringence. More detailed descriptions of the equipment and procedure have been given elsewhere[13,14].

RESULTS AND DISCUSSION

Crystallization behaviour of running filament

The X-ray diffraction curves at 20 cm from the spinneret show a liquid or amorphous halo. At 25 cm from the spinneret, crystalline peaks are recognized in the X-ray diffraction curve. The variation of crystallinity along the spinning path obtained by X-ray diffraction is shown in *Figure 1*. The crystallization begins at a point 22–25 cm from the spinneret, and the degrees of crystallinity at 60–100 cm are similar to that of the take-up fibre. The residence time in the region of rapid development of crystallization is very small, in the order of 0.5–1 sec. At the onset of crystallization, attenuation of the running filament is still in process and the first half of crystallization proceeds under longitudinal deformation. The crystalline orientation factor and the fraction of a^*-axis-oriented crystallite are not changed throughout the crystallization process[13].

The distributions of temperature and molecular orientation of the non-crystalline component (Δn_a) are shown in *Figure 2*. In the initial stage of crystallization, molecular orientation of the non-crystalline component indicates a minimum and negative value such as the results at low elongation of drawing[15,16]. This may be interpreted in terms of loosening of the chain in the non-crystalline part by heat of crystallization[14]. In the final stage of crystallization, the molecular orientation of the non-crystalline component decreases with the progress of crystallization. This can be accounted for by the concentration of strain from progressive crystallites around the non-crystalline chain[14].

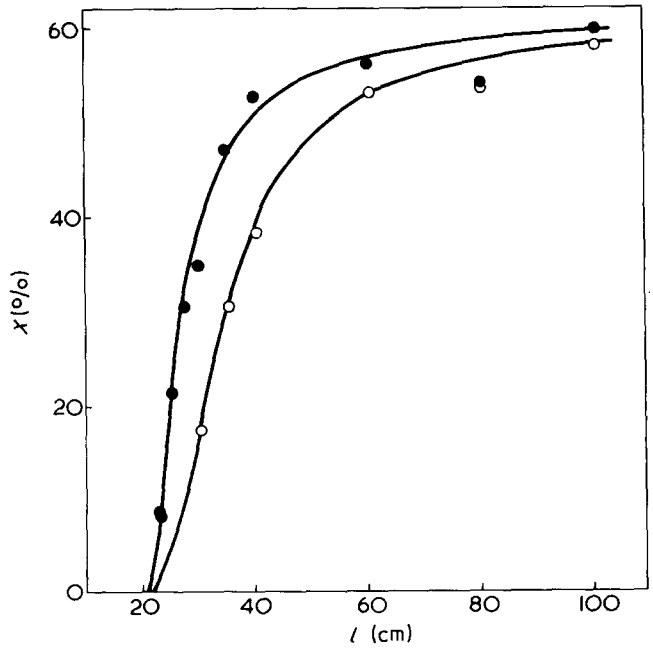

Figure 1 Variation of crystallinity X along the spinning path for take-up velocities of 40 m/min (○) and 10 m/min (●)

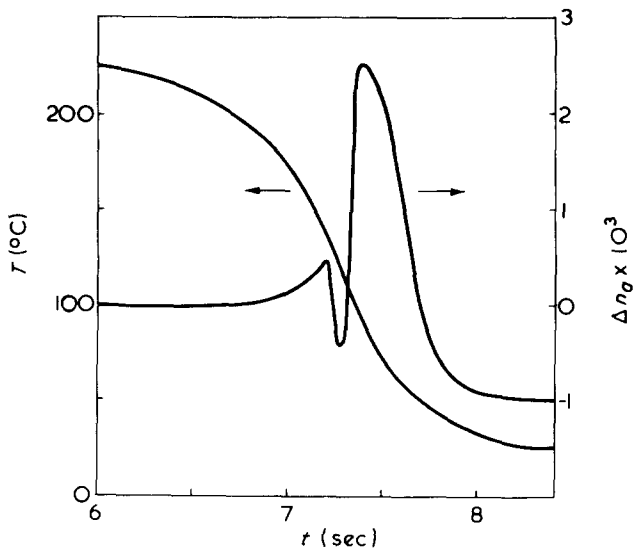

Figure 2 Variation of temperature T and orientation parameter Δn_a of running filament with time from spinneret

Isothermal crystallization of isotropic melt

Isothermal crystallization of an isotropic melt may be the most simplified case of crystallization in running filaments during melt spinning. Two different results have been published for the temperature distribution along the spinning path. One of these is that the heat of crystallization can be neglected[11,17]; the other is that it cannot[18,19]. In the latter, the temperature of the filament is kept constant in the early stages of crystallization because of the balance between heat released by crystallization and that lost by cooling. In the first, we will deal with the early stages of crystallization during melt spinning as an isothermal crystallization.

Figure 3 shows the Avrami plots of $\ln[-\ln(1 - X/X_\infty)]$ against $\ln t$ for take-up velocities (V_E) of 10 m/min and 40 m/min, respectively. Time t of crystallization in the Avrami plots is usually regarded as the time interval from the instant ($t = 0$) when crystallization temperature is attained. For the running filament of melt spinning, however, the determination of that time is very difficult. Four cases in *Figure 3* are chosen as follows: one, $t = 0$ at the time when the filament is cooled to the melting point; the second, $t = 0$ at the time when the crystallization is apparently observed. The others are arbitrarily chosen between these two points. In *Figure 3*, the data points fall upon a straight line for an early stage of crystallization. The results for Avrami's exponent n as functions of the start points in crystallization are summarized in *Table 1* in which the start points are given by the time (t_0) from the spinneret and by the temperature (T_0) of the running filament at this point. Supposing that the start point of crystallization lies in the time when the crystallization is apparently observed, the slopes and the intercepts of these lines give values of $n = 1.1$ and $K = 1.1$ sec^{-1} ($V_E = 10$ m/min) or $K = 2.9$ sec^{-1} ($V_E = 40$ m/min). The exponent $n = 1$ is in agreement with results reported by other investigators for the rate of oriented crystallization of natural rubber[20] and crosslinked polyethylene[21]. This would imply heterogenous nucleation with concurrent one-dimensional linear growth[9]. The values of the crystallization rate constants of a running filament are much higher than those of general crystallization. Moreover the crystallization rate constant at high take-up velocity is larger than that at low take-up velocity. The results show that molecular orientation by extension accelerates crystallization. However, on the assumption that the start point of crystallization is in the time when the filament is cooled to the melting point, the value of $n = 3$ is obtained, which is very similar to the results of isothermal crystallization from an isotropic melt for polypropylene[22–25].

Temperature dependence of crystallization rate constant

Data for crystallization rate constant K and linear growth rate constant G have been reported by several investigators for polypropylene[22–27]. However, the temperature dependence of K and G for polypropylene have not been expressed as a general formula over a wide temperature range. On the other hand, for poly(ethylene succinate), natural rubber and nylon-6, this has been expressed by Takayanagi and Kusumoto[28]. Their method can be used to determine the temperature dependence of K and G from existing data for commercial polypropylene. It was assumed by them that the $(T_m/T)(1/\Delta T)$ law is applicable to the term of the critical nucleus forma-

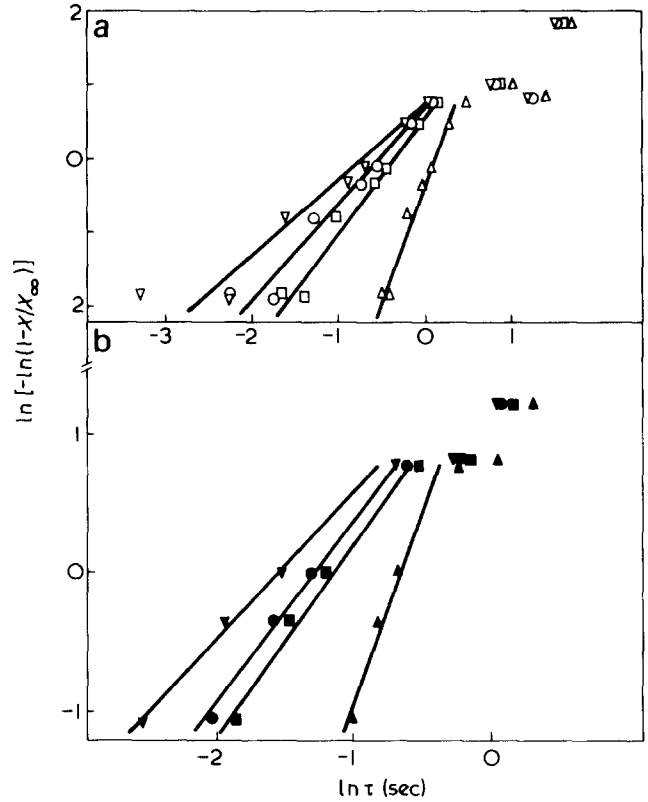

Figure 3 Plot of $\ln(-\ln(1 - X/X_\infty))$ against $\ln\tau$. (a) Take-up velocity 10 m/min; ▽, $t_0 = 9.441$ sec, $T_0 = 155$°C; ○, $t_0 = 9.370$ sec, $T_0 = 159$°C; □, $t_0 = 9.276$ sec, $T_0 = 163$°C; △, $t_0 = 8.863$ sec, $T_0 = 184$°C. (b) Take-up velocity 40 m/min; ▼, $t_0 = 7.223$ sec, $T_0 = 132$°C; ●, $t_0 = 7.168$ sec, $T_0 = 145$°C; ■, $t_0 = 7.147$ sec, $T_0 = 150$°C; ▲, $t_0 = 6.930$ sec, $T_0 = 180$°C

Table 1 Set of n for the start point of crystallization

$V = 10$ m/min			$V = 40$ m/min		
t_0 (sec)	T_0 (°C)	n	t_0 (sec)	T_0 (°C)	n
9.441	155	1.1	7.223	132	1.1
9.370	159	1.3	7.168	145	1.4
9.276	163	1.5	7.147	150	1.5
8.863	184	3.3	6.930	180	3.1

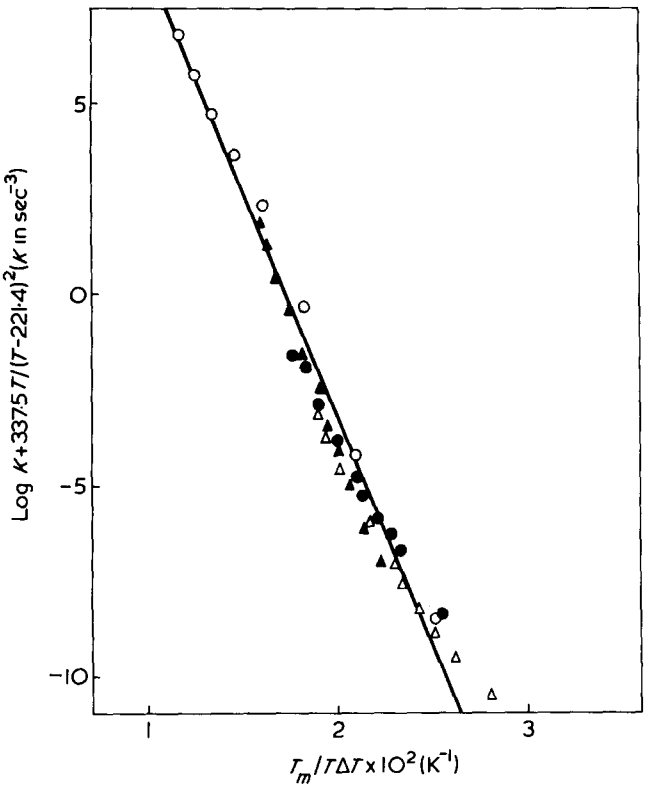

Figure 4 Plot of log $K + 337.5T/(T - 221.4)^2$ *versus* $T_m/T\Delta T$ for commercial PP: ●, Ishizuka[22]; ○, Magil[23]; ▲, Iwanami *et al.*[24]; △, Marker *et al.*[25]

tion and the activation energies for transport across the liquid–crystal interface are proportional to the activation energy of flow obtained from WLF equation. Then the temperature dependences of K, G and $\dot{N}$ can be expressed as:

$$\ln K = \ln K_c - \frac{m\rho C_1 T}{(T - C_2)^2} - \frac{(mC_3 + C_4)T_m}{T\Delta T}$$

$$\ln G = \ln G_c - \frac{\rho C_1 T}{(T - C_2)^2} - \frac{C_3 T_m}{T\Delta T} \qquad (5)$$

$$\ln \dot{N} = \ln \dot{N}_c - \frac{\rho C_1 T}{(T - C_2)^2} - \frac{C_3 T_m}{T\Delta T}$$

where ρ, C_1 and C_2 are constant, m is an integer that depends upon the geometry of the growth process, and C_3 and C_4 are estimated from plots of $\ln K + mC_1T/(T - C_2)^2$ against $T_m/T\Delta T$ and $\ln G + C_1T/(T - C_2)^2$ against $T_m/T\Delta T$. The former plots, from data for commercial polypropylene obtained by several investigators, are illustrated in *Figure 4*. Here, the values of $T_g = 0°C$[29] and $T_m = 184°C$[30] are adopted.

Despite all the points in this figure having been obtained by different methods of many investigators, a straight line may be drawn through the data points. The plots of $\ln G + C_1T/(T - C_2)^2$ against $T_m/T\Delta T$ can be also obtained as a straight line. For the isothermal crystallization of polypropylene, Avrami's exponent $n = 3$ has been reported by several investigators[22–25] and it would imply a heterogeneous nucleation with concurrent three-dimensional growth. In this case $\dot{N}$ in equation (5) can be replaced by the number of heterogeneous nuclei $\bar{N}$ which may be similarly dependent on temperature. Both these results and data are illustrated in *Figure 5*.

Orientation dependence of crystallization rate constnat

Polymer molecules are considered to be deformed by deformation of the polymer melt, and their entropy is usually decreased. The decrease in entropy of the melt allows crystallization to occur at a higher temperature than would normally be observed for the same substance in the absence of any deformation. The effects of G and $\dot{N}$ in such a condition have been evaluated for isothermal crystallization under shear deformation of polyethylene by Kobayashi and Nagasawa[7]. In this section, this theory is applied to uniaxial deformation of polypropylene.

Assuming a Gaussian chain, the orientation and the decrease in entropy for the polymer melt with extension ratio (λ) are given by:

$$\Delta n_a = \frac{2\pi}{45}\frac{(n^2 + 2)^2}{n} N(\alpha_1 - \alpha_2)\left(\lambda^2 - \frac{1}{\lambda}\right) \qquad (6)$$

$$\Delta s_o = -\frac{NK}{2}\left(\lambda^2 + \frac{2}{\lambda} - 3\right) \qquad (7)$$

where n is the mean refractive index of polymer, N is the number of polymer segments per unit volume, and $\alpha_1 - \alpha_2$ is the difference of principal refractive indices. For polypropylene $\alpha_1 - \alpha_2 = 3.602 \times 10^{-25}$, and n and N are given as functions of density.

On the other hand, the melting point (T_{mo}) in an oriented polymer system can be written as:

$$T_{mo} = \frac{\Delta s}{\Delta s - \Delta s_o} T_m \qquad (8)$$

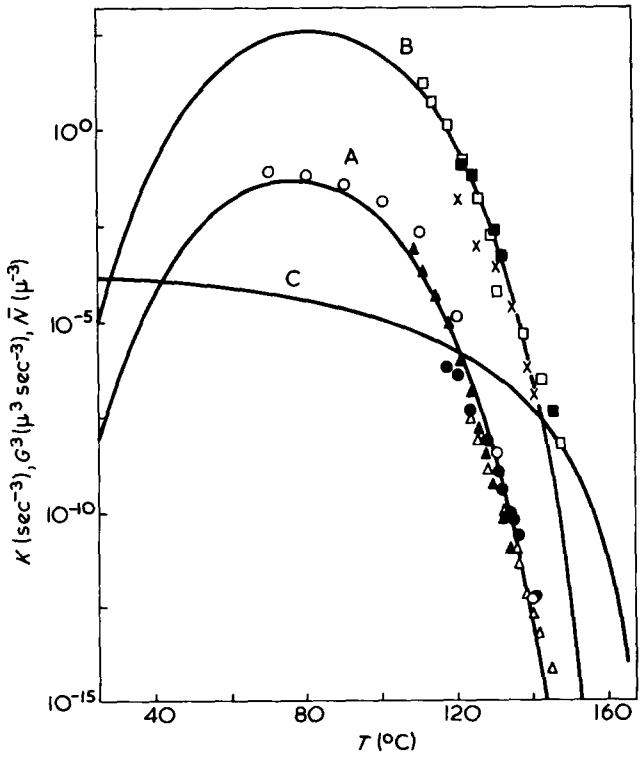

Figure 5 Plots of K (A); G^3 (B) and $\bar{N}$ (C) *versus* crystallization temperature T. ——, calculated from equation (5). ■, Marker *et al.*[25]; □, Padden *et al.*[26]; X, Hoshino *et al.*[27]; other symbols as in *Figure 4*

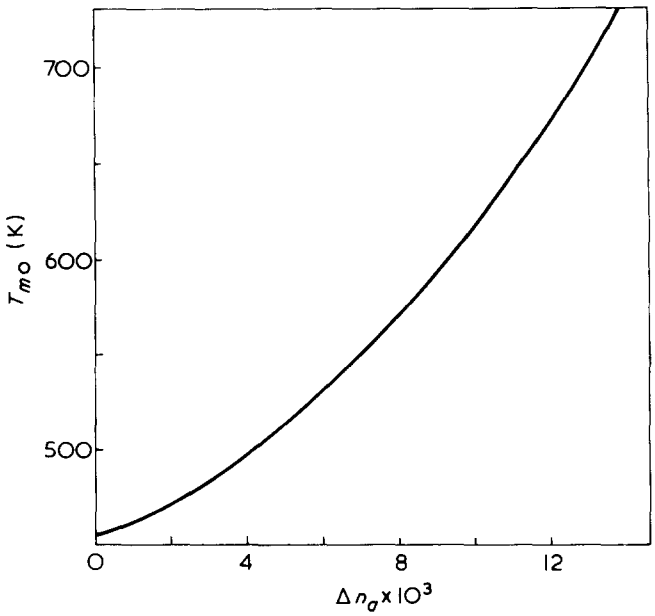

Figure 6 Melting temperature in oriented system of polypropylene as a function of non-crystal orientation parameter Δn_a. The line is calculated from equations (6), (7) and (8)

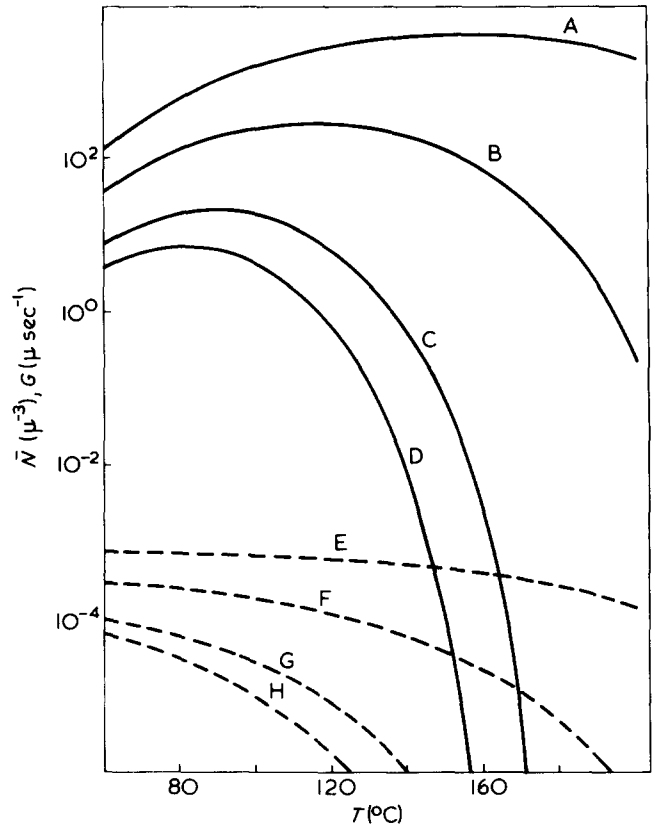

Figure 7 Variation of G (———) and $\bar{N}$ (— — —) with crystallization temperature for various orientation parameters Δn_a: A, E, $\Delta n_a = 10 \times 10^{-3}$; B, F, $\Delta n_a = 5.7 \times 10^{-3}$; C, G, $\Delta n_a = 2.0 \times 10^{-3}$; D,H, $\Delta n_a = 0$

The variation of melting point (T_{mo}) with non-crystalline orientation parameter (Δn_a) is shown in *Figure 6* for $\Delta s = 3.92 \times 10^6$erg/cm^3 °C [30]. By substitution of T_{mo} into equation (5) both the temperature and orientation dependences of $G(T,\Delta n_a)$ and $\bar{N}(T,\Delta n_a)$ can be obtained. These results are plotted against T for several different values of Δn_a in *Figure 7*. If the horizontal axis in *Figure 7* is replaced by Δn_a, it is shown in the Figure that $G(T,\Delta n_a)$ and $\bar{N}(T,\Delta n_a)$ increase with increasing Δn_a.

Non-isothermal crystallization in melt spinning

First, we deal with non-isothermal crystallization of an isotropic melt. The growth rate and the number of nuclei as a function of time from the spinneret can be estimated from combination of *Figure 5* with the variation of temperature in *Figure 2*. Then, assuming that $\Delta n_a(t)$ is zero in equation (4), the degree of crystallinity is calculated along the spinning path. A plot of the calculated values against time from spinneret is shown in *Figure 8* together with the results using the X-ray diffraction method. Here, in calculating these curves, the values of shape factor of equation (4) used are $k_f = 4\pi/3$ for three-dimensional growth, $k_f = \pi l_c$ (l_c = 150 Å) for two-dimensional growth, or $k_f = 1/2\pi d_c^2$ (d_c = 1000 Å) for one-dimensional growth. The calculated curves cannot be reconciled with the experimental data. This suggests that the actual crystallization during melt spinning occurs extremely fast.

In non-isothermal crystallization of an oriented melt, the growth rate and the number of nuclei as a function of time from spinneret can be estimated from combination of *Figure 7* with *Figure 2*. The degree of crystallinity is then calculated by using equation (4). The results are shown in *Figure 8*. The parameters utilized in the calculation are the same as in the case of non-isothermal crystallization of an isotropic melt. The calculated curves are still not fitted by the experimental data. The effect of orientation is apparent, however, by comparison of the results for non-isothermal crystallization in an isotropic melt.

On the other hand, constant molecular orientation of the crystalline component (Δn_c) was obtained throughout the crystallization process[13]. The molecular orientation of the crystalline component was 0.014 for a take-up velo-

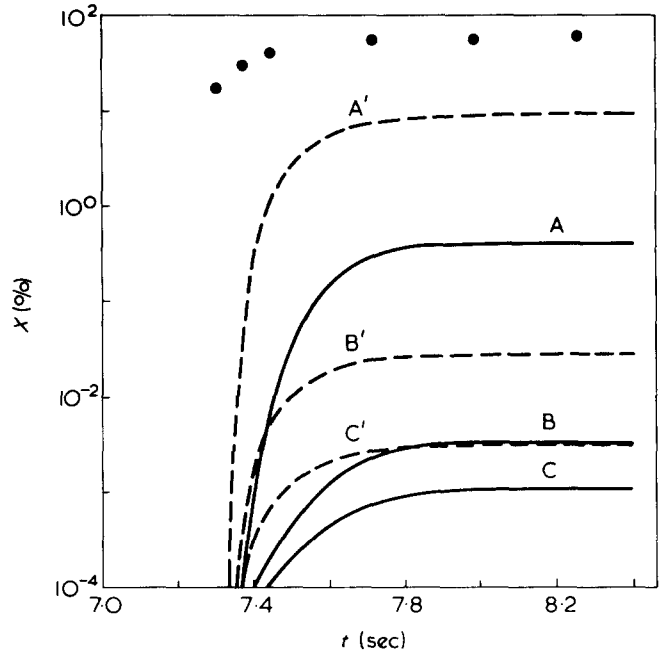

Figure 8 Variation of crystallinity X along the spinning way for experimental data (●), theoretical value (———) in the non-isothermal crystallization of isotropic melt and theoretical value (— — —) in the non-isothermal crystallization of non-isotropic melt; A,A', three-dimensional growth; B,B', two-dimensional growth; C,C', one-dimensional growth

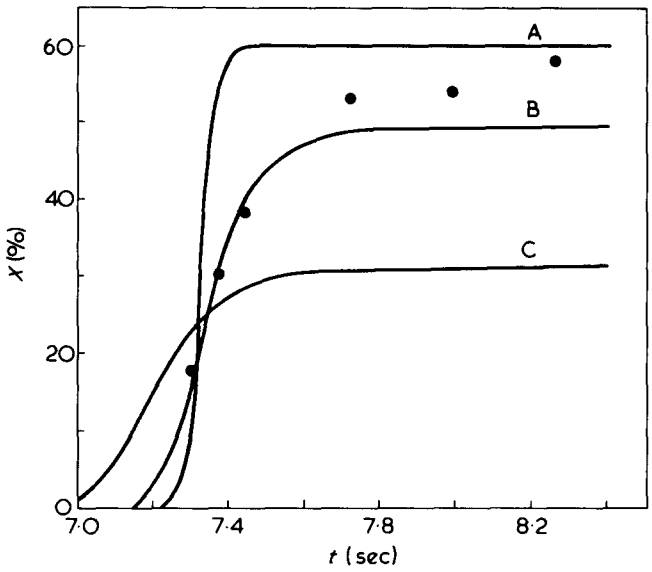

Figure 9 Variation of crystallinity X along the spinning way for experimental data (●) and theoretical value (———) in the non-isothermal crystallization of non-isotropic melt with a constant crystallizable molecular orientation: A, three-dimensional growth, $\Delta n_a = 0.004$; B, two-dimensional growth, $\Delta n_a = 0.0065$; C, one-dimensional growth $\Delta n_a = 0.013$

city of 40 m/min. From this result it may be inferred that the orientation of 'crystallizable molecules' is constant throughtout the crystallization process. The degree of crystallinity is calculated assuming that $\Delta n_a(t)$ is constant in equation (4). The growth rate, and the number of nuclei in the melt with constant orientation, are obtained from *Figure 7* as functions of temperature. The growth rate ($G[T(t), \Delta n_a(t)]$) and the number of nuclei ($\bar{N}[T(t), \Delta n_a(t)]$) at a time t from the spinneret can be estimated from a combination of the temperature dependence with the distribution of temperature along the spinning path in *Figure 2*. Substituting $G[T(t), \Delta n_a(t)]$ and $\bar{N}[T(t), \Delta n_a(t)]$ into equation (4), the degree of crystallinity can be calculated as a function of time from the spinneret. The results are shown in *Figure 9*. Here, in calculating these curves, the following values of non-crystalline molecular orientation and shape factor in equation (4) are used: $\Delta n_a = 0.004$ and $k_f = 4\pi/3$ for three-dimensional growth; $\Delta n_a = 0.0065$ and $k_f = \pi l_c$ ($l_c = 150$ Å) for two-dimensional growth; $\Delta n_a = 0.013$ and $k_f = 1/2\pi d_c^2$ ($d_c = 1000$ Å) for one-dimensional growth. In these molecular orientations, the calculated curves become of the same order as those of experimental data. In particular, crystallization with two-dimensional growth provides the best fit to the experimental data. Then, in the case of non-isothermal crystallization of a non-isotropic melt with highly oriented crystallizable molecules, the calculated value provides a better fit to the experimental data than the other cases (*Figure 8*). Thus these results suggest that a good many nuclei are produced in the initial stage of crystallization and successively only highly oriented molecules can become incorporated into crystallites. In the initial stage of crystallization, however, overall birefringence is very small. That is, only a small part of the supercooled melt can be nucleated and that part has a higher orientation than the other parts. Further, only molecules in the supercooled melt which have orientation comparable to the nucleated crystallites can grow crystallites throughout the crystallization process in melt spinning. Hence, it is found that the crystallization process in melt spinning may be governed by localized molecular orientation of the supercooled melt in the very initial stage.

REFERENCES

1 Ziabicki, A. *Appl. Polym. Symp.* 1967, **6**, 1
2 Ishibashi, T., Aoki, K. and Ishii, T. *Kobunshi Kagaku* 1970, **27**, 186
3 Ozawa, I. *Polymer* 1971, **12**, 150
4 Nakamura, K., Watanabe, T., Katayama, K. and Amano, T. *J. Appl. Polym. Sci.* 1972, **16**, 1077
5 Nakamura, K., Watanabe, T. and Amano, T. *J. Appl. Polym. Sci.* 1973, **17**, 1031
6 Nakamura, K., Watanabe, T., Amano, T. and Katayama, K. *J. Appl. Polym. Sci.* 1974, **18**, 615
7 Kobayashi, K. and Nagasawa, T. *J. Macromol. Sci. (B)* 1970, **4**, 331
8 Avrami, M. *J. Chem. Phys.* 1939, **7**, 1103
9 Avrami, M. *J. Chem. Phys.* 1940, **8**, 212
10 Mandelkern, L. 'Crystallization of Polymers', McGraw-Hill, New York, 1964, Ch. 8
11 Natta, G., Corradini, P. and Cesari, M. *Atti. Accad. Naz. Lincei, Rend. Cl. Sci. Fis. Mat. Nat. Rend.* 1957, **22**, 11
12 Ziabicki, A. 'Man-Made Fibers', Wiley, New York, 1968, Vol 1, Ch 5
13 Ishizuka, O. and Koyama, K. *Sen'i Gakkaishi* 1976, **32**, T43
14 Ishizuka, O. and Koyama, K. *Sen'i Gakkaishi* 1976, **32**, T49
15 Hoshino, S., Powers, J., Legrand, D. G., Kawai, H. and Stein, R. S. *J. Polym. Sci.* 1962, **58**, 185
16 Samuels, R. J. *J. Polym. Sci.* 1965, **3**, 1741
17 Kase, S. and Matsuo, T. *J. Polym. Sci. (A)* 1965. **3**, 2541
18 Katayama, K., Amano, T. and Nakamura, T. *Kolloid-Z* 1968, **226**, 125
19 Spruiell, J. E. and White, J. L. *Appl. Polym. Symp.* 1975, **27**, 121
20 Kim, Hyo-gun and Mandelkern, L. *J. Polym. Sci.* 1967, **6**, 181
21 Kitamaru, R. and Chu, H. D. *Bull. Inst. Chem. Res. Kyoto Univ.* 1968, **46**, 97
22 Ishizuka, O. *Kogyo Kagaku Zasshi* 1962, **65**, 247
23 Magil, J. H. *Polymer* 1962, **3**, 35
24 Iwanami, T., Takai, R. and Kaneko, R. *Kobunshi Kagaku* 1972, **29**, 139
25 Marker, L., Hay, P. M., Tilley, G. P., Early, R. M. and Sweeting, O. J. *J. Polym. Sci.* 1959. **38**, 33
26 Padden, F. J. and Keith, H. D. *J. Appl. Phys.* 1959, **30**, 1479
27 Hoshino, S., Meinecke, E., Powers, J. and Newman, S. *J. Polym. Sci. (A)* 1965, **3**, 3041
28 Takayanagi, M. and Kusumoto, N. *Kogyo Kagaku Zasshi* 1959, **62**, 587
29 Horio, M., Imamura, R., Ishizuka, O. and Fujiwara, H. *13th Ann. Meeting Jpn Chem. Soc. Tokyo 1960* p 400
30 Danusso. F. and Gianotti, G. *Eur. Polym. J.* 1968, **4**, 165